Proceedings Paper:

Henthorn, S.D., Ford, K.L. orcid.org/0000-0002-1080-6193 and O'Farrell, T. (2018) A low-loss reconfigurable frequency selective surface based antenna for direct antenna modulation. In: Antennas & Propagation Conference (LAPC 2017), Loughborough. Antennas & Propagation Conference (LAPC 2017), Loughborough, 13-14 Nov 2017, Loughborough, UK. IET . ISBN 978-1-78561-700-3

https://doi.org/10.1049/cp.2017.0233

A low-loss reconfigurable Frequency Selective Surface based antenna for Direct Antenna Modulation

Stephen Henthorn, Kenneth Lee Ford, Timothy O'Farrell

Dept. of Electronic and Electrical Engineering, University of Sheffield, Sheffield, United Kingdom, sdhenthorn1@sheffield.ac.uk

Keywords: Frequency selective surfaces, Direct antenna modulation, Phase shift keying, reconfigurable antennas

Abstract

A directly modulating antenna incorporating a reconfigurable Frequency Selective Surface (FSS) for arbitrary phase modulation is designed and simulated. A 4-layer FSS is used to minimise constellation distortion, with only 1.5dB variation in transmitted magnitude for 360^o phase change. Low loss substrates and Barium Strontium Titante (BST) variable capacitors are simulated to reduce the antenna loss to 1.3dB in the filter pass band and achieve an average total efficiency of 65% when producing an 8-PSK constellation.

1 Introduction

Modern communications systems make use of complex digital modulation schemes, producing waveforms which are broadband and often have significant peak to average power ratios (PAPRs). In conventional transmitters, this places a requirement on the power amplifier (PA) to be linear across the input power and frequency ranges in order to avoid distorting the signal [1]. This often results in the PA being operated at back-off from its saturation point, reducing the power efficiency significantly. Recently, considerable effort has been made to improve efficiency and reduce distortion, including PA designs such as the Doherty amplifier [2], and predistortion of the signal [3], both of which add complexity to the transmitter.

A recent approach to the problem is Direct Antenna Modulation (DAM), where an amplified carrier wave is modulated at the antenna. This means only the carrier wave is amplified, rather than the broadband modulated waveform, allowing the PA to operate in its efficient non-linear region without adding distortion. Several approaches have been taken, including integrating active components into the antenna to produce simple modulation schemes [4], or surrounding the antenna by passive switched reflectors to produce directional complex modulation [5]. We recently, [6], proposed an antenna loaded with a three-layer reconfigurable Frequency Selective Surface (FSS), using varactor diodes to vary the FSS centre frequency, and hence the transmitted phase from the antenna (Fig. 1). Its performance as a modulator is evaluated in an end-to-end Quadrature Phase Shift Keying (QPSK) communications system in [7].

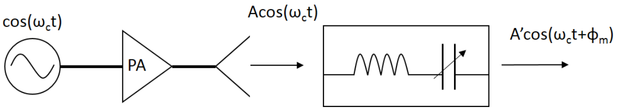

Fig. 1: Concept of a DAM modulator using an FSS

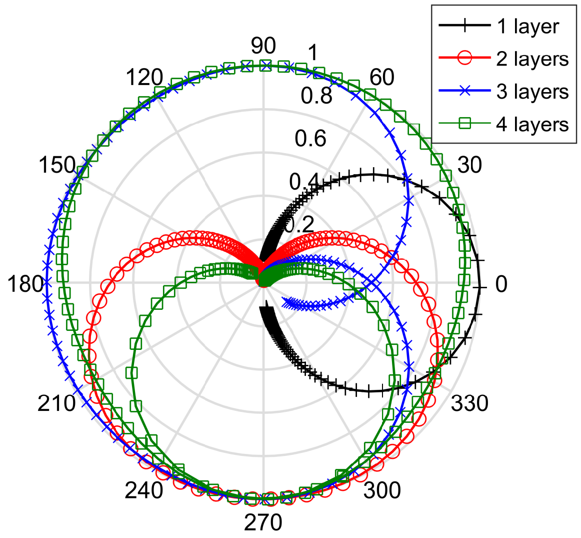

Fig. 2: Polar plot of transmitted signal of LC bandpass filters of different orders with changing capacitance

This paper further develops the work of [7], presenting an DAM for QPSK, continuous phase and polyphase signals [8]. The design uses low-loss materials and devices to improve the antenna efficiency, and a 4-layer FSS for an improved modulation performance. The antenna design and its performance as an antenna and a modulator are discussed.

2 Frequency Selective Surface design

The reconfigurable FSS for a PSK modulating antenna should be broadband, such that there is little change in transmitted magnitude across 360° of change in transmitted phase. To achieve this, multiple layers of FSS are required. This is demonstrated in Fig. 2, where the magnitude and phase transmitted through different numbers of layers of LC bandpass FSS are shown with changing capacitance at a fixed frequency.

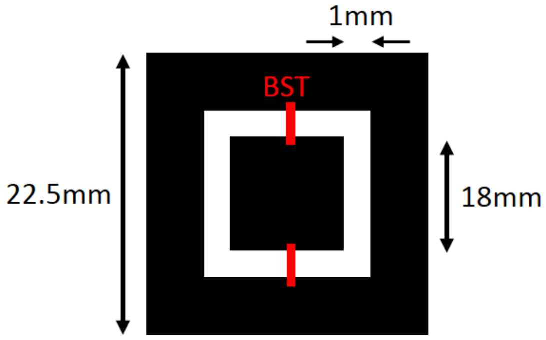

Fig. 3: FSS unit cell design

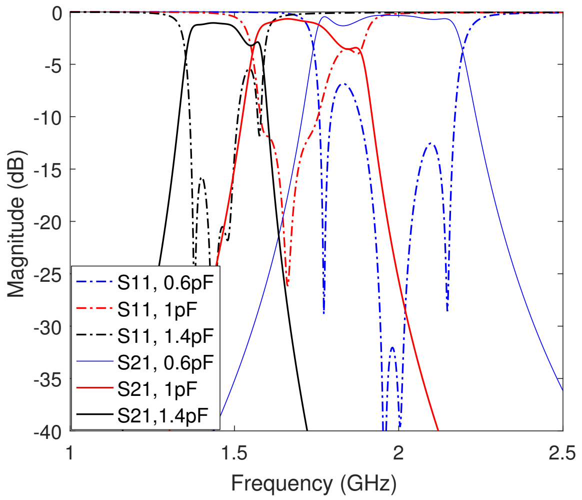

Fig. 4: Reflection and transmission coefficients of FSS design in free space

The 4 layer design was selected as it provides a maximum of less than 1dB variation around the whole constellation, and in a real system there is a trade-off with loss increasing linearly with the number of layers.

A square-loop aperture design for the FSS was chosen for its stability with angle of incidence, its relatively broadband frequency response and its ease of implementation. The unit cell geometry was designed using the square-loop design equations in [9] and Babinet's principle. In order for the FSS to resonate at 1.8GHz when variable capacitors are integrated, the geometry was designed for 3.4GHz. The design in Fig. 3, produces an equivalent inductance and capacitance of 24pH and 93pF, respectively.

The design was validated in CST Microwave Studio, using Floquet boundaries in free space to simulate four infinite FSS spaced by $\lambda_0/4$. The unit cell geometry was simulated as PEC, and each layer had a 1.6mm TLY5 fibreglass substrate, chosen for its low loss tangent at microwave frequencies ($\epsilon_r 2.2, tan\delta = 0.0009$). Variable capacitors were integrated across the gaps in the unit cell to allow tuning of the FSS to produce modulation. STPTIC-27G2 variable capacitors, which are based on a Barium Strontium Titanate material, were chosen for their high Q-factor at the frequency of interest and good linearity [10]. The capacitors were simulated as lumped elements with a tuning range of 0.6 to 3pF and an Equivalent Series Resistance (ESR) of 0.6Ω. However, only the lower half of the capacitance range is explored, as increasing C increases the current through the variable capacitor, leading to higher resistive losses in the component. This is marginally offset by a lower ESR for a similar Q-factor at larger capacitances, but losses through the surfaces were found to still increase. The simulation shows between 1.1dB and 0.3dB minimum transmission loss at various capacitances (Fig. 4).

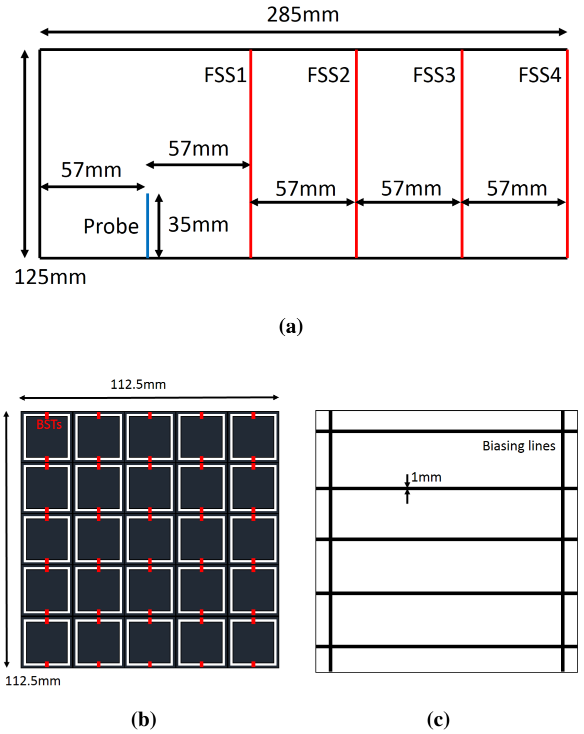

(a)

(b)

(c)

Fig. 5: (a) Side-on view of final antenna design, (b) Front-on view of antenna design, (c) Reverse of each FSS layer

3 DAM Antenna design

To ensure all fields pass through all layers of the FSS and to limit the antenna form factor, the FSS was integrated into a cavity-backed antenna with a monopole feed (Fig. 5a). This increases the centre frequency of the FSS by 350MHz compared with the FSS in free space. Each layer consists of a 5×5 grid of unit cells (Fig. 5b), allowing the cavity to be large enough to propagate fields at 1.8GHz while restricting higher order modes. As the FSS is no longer in free space, a layer spacing of $\lambda_0/4 = 41.7$mm will not produce an optimum filter response at the operating frequency. However, as the cavity is not an infinite length waveguide, the theoretically

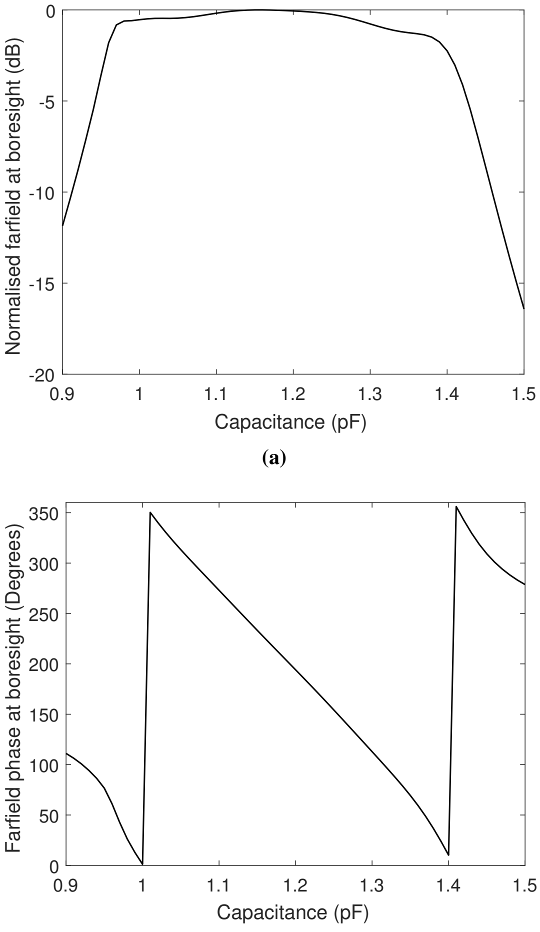

(a)

(b)

Fig. 6: (a) Magnitude and (b) phase variation of E-field at boresight in the farfield with varying capacitance

derived guide quarter-wavelength, $\lambda_g/4 = 76$mm, also does not produce an optimal filter. Simulation in CST found that a spacing of $\lambda_s/4 = 57$mm gives an optimally flat filter response at 1.8GHz. The capacitors are modelled as before, and are placed in alignment with the antenna E-field to minimise the number of components required. 1mm wide bias lines are modelled on the reverse of the FSS substrate, and are mostly orthogonal to the cavity E-field, with the two vertical lines toward the edges of the antenna to minimise their effect on the transmitted signal, as shown in Fig. 5c.

4 Antenna performance

The full antenna was simulated in CST Microwave Studio. Fig.6 shows the boresight normalised farfield magnitude and phase received at 1.8GHz with changing capacitance. It shows a nearly flat magnitude response between 0.97 and 1.39pF, with a highly linear phase change in this region. Between 0.97 and 1.38pF, there is 360° of phase change for only 1.5dB variation in magnitude, giving the maximum difference in magnitude between two arbitrary PSK constellation points.

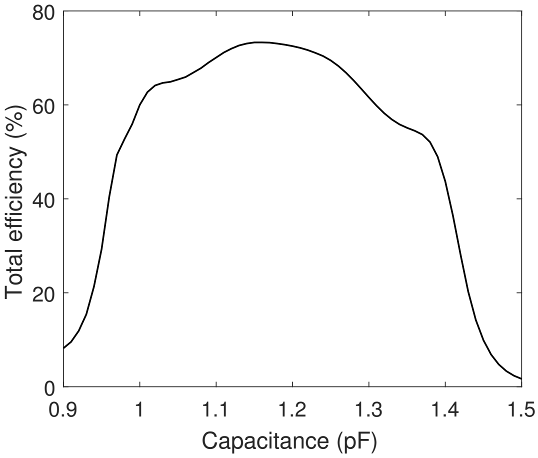

Fig. 7: Total simulated efficiency of antenna with varying capacitance

The total efficiency of the antenna is simulated as varying between 54.5% and 73% in the filter pass region, with a mean of 65% (Fig. 7). Losses occur in the substrate and the parasitic resistance of the variable capacitors. However, at 0.98pF, there is a decrease in antenna efficiency but an increase in the magnitude of the signal received at boresight. This is due to an increase in peak directivity at this point. As such, the constellation in directions other than boresight must be considered when selecting constellation patterns, as reflected non-Line-of-Sight (LoS) paths with a distorted constellation may interfere in a less determinate way with a boresight constellation at a receiver. Fig. 8 shows an 8-PSK constellation at various observation angles within the maximum 3dB beamwidth, 80°, in both E- and H-planes, where each complete constellation is normalised. The constellation is completely stable in the H-plane, and the different points have only 14% variation in absolute amplitude. In the E-plane, there is more variation, with up to 26% difference in amplitude and 11° in phase at a viewing angle of 40°. However, this constellation is transmitted with 3dB less power than the boresight constellation, so any interference from reflected impaired constellations should be small.

5 Conclusion

A directly phase modulating antenna incorporating a reconfigurable FSS has been designed and simulated. The design is simulated as able to produce an 8-PSK constellation with only 14% variation in constellation magnitude. The antenna loss is 1.3dB in the filter pass band and achieves an average total efficiency of 65% across an 8-PSK constellation.

Acknowledgements

This work is funded by an EPSRC iCASE award with industrial partners NEC and BT. The data for this work can be accessed at https://figshare.com/s/96c1f68ee99a868ee1b2.

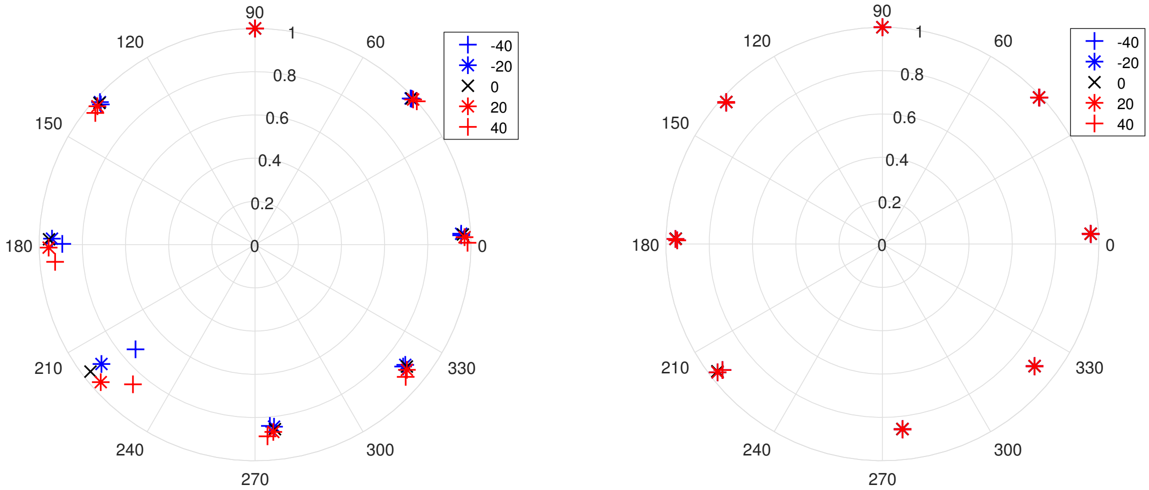

(a) (b)

Fig. 8: Simulated 8-PSK constellation from antenna at various observation angles in (a) E-plane (b) H-plane

References

[1] Raghavan, A., Srirattana, N., Laskar, J.: "Modeling and Design Techniques for RF Power Amplifiers", (Wiley-IEEE Press, 2008)

[2] Raghavan, A., Srirattana, N., Laskar, J.: "Efficiency Enhancement of RF Power Amplifiers", in 'Modeling and Design Techniques for RF Power Amplifiers' (Wiley-IEEE Press, 2008), pp 173–198.

[3] Lei, D., Zhou, G. T., Morgan, D. R., Ma Zhengxiang, Kenney, J. S., Jaehyeong, K., Giardina, C. R. "A robust digital baseband predistorter constructed using memory polynomials", *IEEE Transactions on Communications*, **52,** pp. 159-165, (2004).

[4] Daehee, P., Minhoe, K., Dong-Ho, C. "Novel single-RF MIMO system based on repetitive Pulse Width Modulation", *IEEE Communications Letters*, **20,** pp. 165–168, (2016).

[5] Babakhani, A., Rutledge, D. B., Hajimiri, A. "Transmitter architectures based on near-field Direct Antenna Modulation", *IEEE Journal of Solid-State Circuits*, **43,** 2674–2692, (2008).

2017 11th European Conference on Antennas and Propagation (EUCAP), Paris, France, 2017, pp. 731-734.

[6] Henthorn, S., Ford, K. L., O'Farrell, T. "Frequency Selective Surface loaded antenna for Direct Antenna Modulation", *2017 11th European Conference on Antennas and Propagation (EUCAP)*, Paris, France, (2017), pp. 731-734.

[7] Henthorn, S., Ford, K. L., O'Farrell, T. "Bit error rate performance of quadrature modulation transmission using reconfigurable Frequency Selective Surfaces", *IEEE Antennas and Wireless Propagation Letters*, **PP(99)**, pp. 1–1, (2017).

[8] O'Farrell, T. "New signature code sequence design techniques for CDMA systems", *Electronics Letters*, **27**, pp. 371–373, (1991).

[9] Langley, R. J., Parker, E. A. "Equivalent circuit model for arrays of square loops", *Electronics Letters*, **18**, pp. 294–296, (1982).

[10] STMicroelectronics. "STPTIC-27G2 Parascan tunable integrated capacitor", *http://www.st.com/content/ccc/resource/technical/-document/datasheet/3a/d0/ac/4a/ab/72/46/aa/-DM00217084.pdf/files/DM00217084.pdf/jcr:content/-translations/en.DM00217084.pdf*, accessed 23 May 2017.